Development of green cement from solid wastes

Shipeng Zhang, Hanxiong Lyu, Peiliang Shen, Lu Zhu and Chi Sun Poon
Department of Civil and Environmental Engineering & Research Centre for Resources Engineering towards Carbon Neutrality, The Hong Kong Polytechnic University, Hong Kong, People's Republic of China

ABSTRACT

In this study, a green cement (GC) was prepared primarily using incineration bottom ash (IBA) and recycled concrete fine (RCF) at a low clinkering temperature of 1200ºC. This clinker mainly consisted of belite (C_2S) and rankinite (C_3S_2) and demonstrated the versatility of strong carbonation reactivity and latent hydraulicity. Compared to the commercial benchmark - ordinary Portland cement - after being subjected to carbonation curing, GC exhibited superior macro- and micro-mechanical performance due to the densified microstructure. In addition to rapid strength gain at an early age, the carbonated GC also exhibited a substantial increase in strength at later ages and eventually recorded a high strength of 86.4 MPa. Furthermore, the leaching behaviour assessment on commonly regulated heavy metals validated the environmental stability of this waste-derived binder. The development of this sustainable cement has good potential to divert solid wastes otherwise destined for landfill sites to high-value-added construction products.

KEYWORDS Incineration bottom ash; recycled concrete fine; sustainable binder; carbonation curing; CO_2 sequestration
CONTACT Shipeng Zhang shipeng.zhang@polyu.edu.hk
Received 25 July 2023

1. Introduction

Municipal solid waste (MSW) and construction/demolition (C&D) waste are two major waste streams in Hong Kong. Compared to other megacities that have developed diverse solid waste disposal methods, Hong Kong mainly relies on three strategic landfill sites for disposal of the city's solid wastes, and all the landfill sites are approaching their design capacities. In view of this, modern treatment and recycling methods have been gradually adopted by the government.

For instance, an Integrated Waste Management Facility (IWMF) is under construction in Hong Kong to address the MSW problem by incinerating waste. Although incineration can reduce the weight, volume, and toxicity of the MSW (Makarichi et al., 2018), it is not an end-of-pipe solution due to the substantial generation of residues, particularly incineration bottom ash (IBA), which accounts for around 20 wt% of the initial weight of the MSW (Yan et al., 2020). According to government information, once IWMF starts operation in 2025, 600 tonnes of IBA will be generated daily. Although attempts have been made to use IBA as low-value construction materials, such as aggregates for fill and road subbase, the potential heavy metal leaching problem, chemical stability issue, and low crushing strength of IBA restrict its application (Baldwin et al., 1997; Schafer et al., 2019).

Similarly, recycled concrete aggregate can be recycled from demolition concrete waste. However, the classic recycling process involving a crushing action by a jaw or impact crushers generates 20 wt% of recycled concrete fines (RCF) that are unsuitable for reuse in new concrete products (Xiao et al., 2018). RCF has a high old cement paste content with higher water absorption, lower density, and poor abrasion resistance than natural aggregates, leading to inferior mechanical and durability performance when incorporated into new concrete (Xuan et al., 2016). Thus, like most anthropogenic solid wastes, the common final destination for IBA and RCF is landfill sites, which inevitably entails the long-term use of precious land resources, and the possibility of ecological risks due to water pollution (Saikia and Kojima, 2006).

Apart from the generation of solid wastes, the massive emission of anthropogenic CO_2 is another severe global environmental challenge (Caldeira and Wickett, 2003; Solomon et al., 2009), which leads to climate change and the associated more frequent extreme weather, such as intense drought, storms, heat waves, rising sea levels, etc. The use of concrete in the construction industry contributes 9% of the total greenhouse gas emissions (OECD, 2019), of which 7-8% are from the cement-making process (Cadavid-Giraldo et al., 2020). The production process of cement clinkers accounts for most of the CO_2 emissions in cement manufacturing, where 30% of CO_2 released can be attributed to fuel combustion and 70% to the decalcination of limestone to lime, an essential constituent in the raw feed of the cement clinkering process (Rodriguez et al., 2011). Advanced combustion systems have been developed for modern cement plants and it is hard to further increase the fuel-burning efficiency (Hasanbeigi et al., 2012). Therefore, reducing the calcium carbonate content in the raw feed and lowering the clinkering temperature are more feasible directions to mitigate the environmental impact of the cement sector.

From a compositional point of view, IBA and RCF can serve as low-carbon mineral sources of lime, silica,

*The first author who was at the age of 35 or below on the closing date of submission for the HKIE Outstanding Paper Award for Young Engineers / Researchers 2023.

and alumina, and iron potentially qualifies as a raw feed for cement making (Clavier et al., 2020; Clavier et al., 2021). To reduce the carbon footprint of cement and utilise solid wastes, numerous studies have been performed to utilise either IBA or RCF in traditional ordinary Portland cement (OPC) making. But only a limited amount of the waste can be used in the raw feeds. Washed IBA can be used as a minor raw material in clinker production, and clinker with mineralogical compositions that are comparable to conventional cement was developed by adding up to 8% IBA as the raw feed (Clavier et al., 2021). A clinker with a reasonable amount of tricalcium silicate (C_3S) content (a primary mineral phase in OPC) was also produced by using 2-6% IBA in the raw feed (Krammart and Tangtermsirikul, 2004); however, the C_3S content decreased with a higher dose of IBA, while dicalcium silicate (C_2S) formation was promoted instead (Krammart and Tangtermsirikul, 2004; Shih et al., 2003). With a replacement ratio of 15%, RCF could be used in Portland cement clinker production at 1450°C without any significant influence on the mineralogy of the final clinker (Schoon et al., 2015). Gastaldi et al. (2015) further increased the RCF incorporation ratio to 55%, and they found that a higher dosage of RCF hindered the formation of C_3S and led to a C_2S-rich clinker. Seemingly, applying a high dosage of RCF or IBA as raw feeds in conventional OPC making has a potential stunting effect on the formation of C_3S, mainly due to the reduced amount of calcium.

In addition, lowering the clinkering temperature also restricts the formation of C_3S. In typical OPC produced at 1450°C, the major clinker phases are C_3S (alite 60%); C_2S (belite 16%); C_3A (aluminate 10%); C_4AF (ferrite 8%) (Hewlett and Liska, 2019). C_3S is the most important constituent of OPC, contributing the majority of the strength of the hydrated cement. Lowering the OPC clinkering temperature would decrease the formation of C_3S, but result in the favourable formation of latent hydraulic or even non-hydraulic calcium silicate phases, such as different polymorphs of C_2S, C_3S_2, and CS (Hewlett and Liska, 2019). However, these phases can be extensively activated by carbonation with CO_2 for strength development. Pure C_2S is the most reactive phase, followed by C_3S, C_3S_2, and CS, and research has confirmed that sole C_2S could achieve a high strength of more than 70 MPa after carbonation (Mu et al., 2019).

This study explored the feasibility of using both IBA and RCF as primary raw feeds to produce a novel green cement (GC) at a low clinkering temperature of 1200°C. Unlike traditional OPC cement with C_3S as the primary clinker phase, C_2S and C_3S_2 were the targeted minerals. The GC was evaluated by a series of analytical investigations, including mineral compositional analysis, macro- and micro-scale mechanical properties tests, thermogravimetric analysis, microstructural morphology analysis, and leaching risk assessment. With the implementation of carbonation curing, the embodied CO_2 of this sustainable binder was significantly reduced in regard to three aspects: (1) low clinkering temperature; (2) low embodied-carbon solid wastes as raw materials; and (3) active CO_2 sequestration during carbonation curing.

2. Materials and methods

2.1. Materials

IBA was obtained from an incinerator in mainland China. Ordinary Portland cement (OPC, CEM I 52.5N) was provided by a local source. RCF was simulated in the laboratory using a 60-day hydrated cement paste prepared with a water/cement ratio of 0.48. Commercially sourced pure CaO was used to adjust the overall composition of the raw feeds. All raw materials were dried and pulverised to a powder form. X-ray fluorescence (XRF, Rigaku Supermini200) characterisation was used to analyse the oxide composition of IBA, RCF, and OPC, as shown in Table 1. Figure 1 shows the particle size distributions of the pulverised IBA, RCF, CaO, and OPC detected by the Malvern Mastersizer 3000.

Table 1. Oxide composition of IBA, RCF and OPC (wt%).

	IBA	RCF	OPC
CaO	14.7	66.5	66.9
SiO_2	56.1	19.7	18.4
Al_2O_3	9.46	5.34	5.36
Fe_2O_3	5.64	3.18	2.95
Na_2O	4.7	-	-
MgO	1.59	1.2	0.628
P_2O_5	2.68	0.18	0.141
SO_3	0.721	2.79	4.46
Cl	0.839	0.0119	
K_2O	1.89	0.656	0.706
TiO_2	0.761	0.292	0.281
Cr_2O_3	0.127	-	-
MnO	0.133	0.067	0.046
NiO	0.043	-	-
CuO	0.159	0.0232	0.0179
ZnO	0.285	0.0268	0.0208
Br	0.0092	-	-
Rb_2O	0.0121	-	-
SrO	0.0447	0.106	0.0952
ZrO_2	0.0589	0.0056	-
PbO	0.0363	-	-
LOI(950)	5.01	20.75	2.37

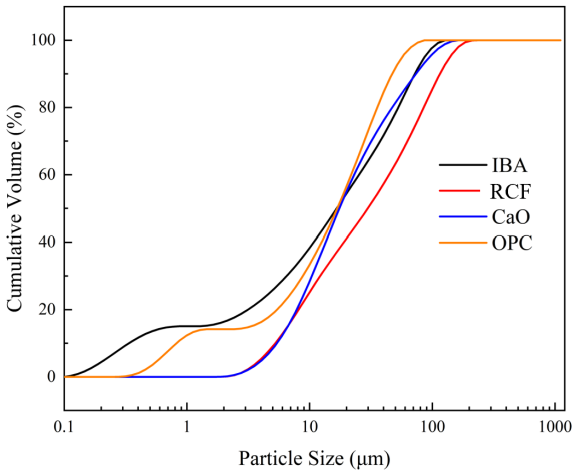

Figure 1. Particle size distributions of IBA, RCF, CaO and OPC.

2.2. Green cement clinkering and mineralogical composition

A targeted raw feed composition was deduced based on the metallurgical thermodynamics of belite formation (Hasegawa, 2014) and multiple trials. The final optimised mixing ratio by weight of the three feed components of IBA, RCF, and CaO was 37.5:48.0:14.5, evaluated based on the preliminary criteria of strength development and carbonation degree. After thoroughly mixing and pressing them into compacts, the raw feeds were clinkered at 1200°C for 2 hours. The cooled-down clinkers were then pulverised into powder to produce the GC. The particle size distribution and specific surface area of GC and OPC are listed in Table 2. Figure 2 shows the light-yellow GC powder and its mineral compositions detected by quantitative X-ray diffraction (QXRD). As expected, belite was produced as a main mineral phase, accompanied by rankinite and gehlenite.

Table 2. Particle size distribution and specific surface area of GC and OPC.

	D10 (μm)	D50 (μm)	D90 (μm)	Specific surface area (m^2/kg)
GC	2.46	21.0	86.7	659.8
OPC	2.48	16.34	45.98	938.0

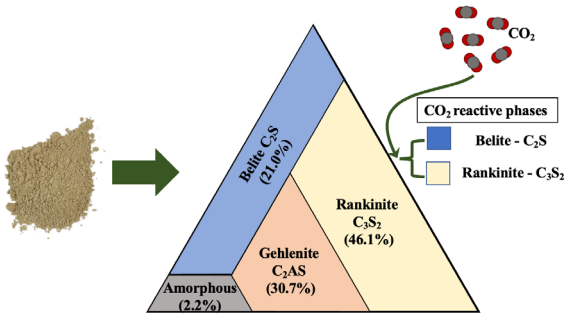

Figure 2. GC and its final mineral compositions.

2.3. Cement paste: sample preparation and curing scenarios

Cement paste cylinders (20 mm in diameter and 15 mm in height) were chosen to be the testing subject by mechanically compacting the GC powder under a unidirectional force of 3 kN into a specially designed stainless-steel mould. The compaction method to fabricate paste samples has been widely applied in research investigating the carbonation reactivities of the C_2S mineral phase (Zhao et al., 2020) and the carbonation hardening of OPC (Zajac et al., 2022). The final water-to-binder ratio was kept at a constant of 0.15 by mass, which is an optimal parameter to prevent water loss during the compacting process, thus resulting in a zero-slump dry paste. This was to allow the presence of air voids between the cement particles in the freshly prepared paste to facilitate CO_2 diffusion. The proportioned clinker powder and water were put into a bowl, and stirred quickly by a mixer to evenly wet the powder surface. OPC pastes were the reference, prepared by the same procedures. After demoulding, the samples were subjected to different curing regimes.

Regular hydration (water) curing (H) and accelerated carbonation curing (C) were used in this work. For the hydration curing, the paste samples were cured in an environmental chamber with 100% relative humidity and at room temperature (25°C) for one day, 28 days, and 60 days. Unlike curing with immersion in water, this method avoids the leaching of portlandite. For carbonation curing, the specimens were cured in an airtight vessel containing pure CO_2 (99.5%) for one day under two bar pressure controlled by a pressure regulator. After one day of carbonation curing, the paste samples could be uniformly carbonated, as shown in Figure 3, with testing of the alkalinity of the sample cross-section by spraying phenolphthalein. A colourless result was observed on the cross-section of the specimen, indicating that the alkalinity was less than 10. All carbonated samples were subjected to further hydration curing to assess the long-term strength.

Figure 3. Phenolphthalein sprayed cross-section of a specimen.

2.4. Characterisations

2.4.1. Carbon sequestration degree

The mass of the paste samples was measured before and after carbonation. The degree of carbonation was determined by the amount of CO_2 uptake, calculated based on the mass gain method (Monkman and Shao, 2006) described in Equation (1).

$$CO_2\ uptake\ (\%) = \frac{M_{after\ carbonation} - M_{before\ carbonation} + M_{water\ lost}}{M_{cement}}, \quad (1)$$

where $M_{after\ carbonation}$ and $M_{before\ carbonation}$ represent the mass of the sample after and before carbonation, respectively; $M_{water\ lost}$ equals the mass of the water lost in the chamber; M_{cement} is the mass of dry cement for preparing a specimen.

2.4.2. Macro- and micro-scale mechanical properties

The compressive strength of the paste samples was determined by a Testometric X500-50 compressing machine. Three values were averaged for each batch. The micro-mechanical properties of the cured samples were characterised by a nanoindenter (Hysitron TI Premier with a three-sided pyramid Berkovich tip, Bruker). The specimens for the nanoindentation test were obtained by first immersion in an epoxy resin, followed by graded polishing, and finally ultrasonic cleaning in alcohol. During the nanoindentation test, loading, holding, and unloading in a trapezoidal loading function lasted for 10 seconds, 5 seconds, and 10 seconds, respectively. The maximum load was 2000 μN. A grid spacing of 10 μm was chosen to avoid mutual interference between the testing areas. A separate zone with 10×10 grids was selected, meaning that 100 indent points were recorded for each specimen. The indentation modulus (E_r) of each indent point was derived from the load-depth curve.

2.4.3. Mineralogy, microstructure and morphology

The mineralogical analysis of the raw and cured cement paste specimens pulverised to a powder was performed by quantitative X-ray diffraction (QXRD, Rigaku Smart-Lab) equipped with Cu-Kα radiation (λ = 1.54 Å) at a voltage of 45 kV and a current of 200 mA over a range of 5-70° with a step size of 0.02°. 10 wt% corundum was used as the internal standard, and the quantitative values were obtained through Rietveld refinement.

After the compression strength test, the crushed fragments were ground into a powder and used for microstructural analysis by using FTIR (model PerkinElmer UATR Two) in the range of 400-4000cm^{-1}, and a thermogravimetry analyser (Rigaku, Thermo plus EVO2). For the thermogravimetric analysis (TGA), the selected samples were heated from 30°C to 900°C with a heating rate of 10°C/min under N_2.

The morphology of fractured surfaces of the specimens was observed by a scanning electron microscope (SEM, Tescan VEGA 3) equipped with an energy-dispersive X-ray (EDX) at a 20 kV accelerating voltage.

2.4.4. Leaching behaviour

The Toxicity Characteristic Leaching Procedure (TCLP, US EPA Method 1311) was conducted on the raw materials and the cement paste samples (cured for 1 day) for environmental risk evaluation. An ICP-OES (SpectroBlue) was used to measure the concentrations of the regulated heavy metals in the TCLP leachate.

3. Results and discussion

3.1. Compressive strength and CO_2 uptake

Figure 4 shows the averaged compressive strength of the hydrated (GC-H) and carbonated GC (GC-C) cement pastes cured for different periods of time. OPC-H represents the strength-over-time profile of the typical commercial OPC cement subject to regular hydration curing. At the same time, OPC-C is the carbonation-curing scenario. As expected, GC only exhibited latent strength gains at later ages. Almost no strength could be detected after one day, and the strength gradually increased to 21.0 MPa at 60 days.

Carbonation, however, could trigger the reactivity of the clinker phases in both the OPC and GC cement systems. As a result, GC recorded a better carbon sequestering ability (CO_2 uptake) of 10.12% than the 8.68% for the carbonated OPC. Meanwhile, carbonation accelerated the strength gain for both binders, particularly for the GC batch. After one day of carbonation curing, the compressive strength of OPC-C underwent an increase of 54.3% compared to OPC-H, reaching 43.9 MPa. For GC-C, its one-day strength

reached 67.8 MPa. The GC-C had the highest compressive strength at all testing ages, and this batch eventually reached 86.4 MPa after one day of carbonation curing and 59 days of hydration curing. Since the carbonation curing methodology involves the usage of a pressurised chamber, it would not be suitable for wet-cast concrete. However, this method favours rapid strength gain and resilience improvement of dry-cast concrete fabricated with a low water/binder ratio, thereby realising the quick demoulding and dismantling of formworks after compaction fabrication. Green cement with carbonation reactivities would present advantages in the production of retaining walls, pavers, and blocks.

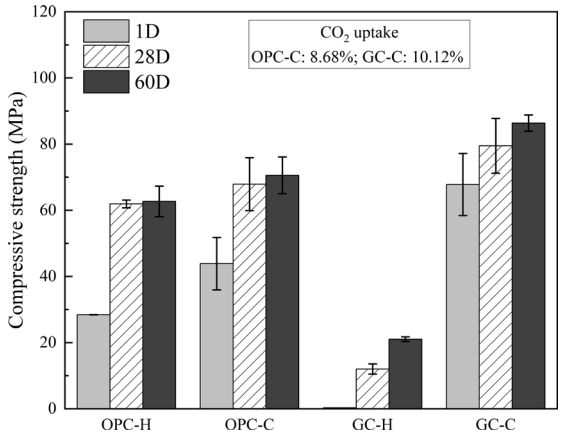

Figure 4. Compressive strength of hydrated and carbonated cement pastes.

3.2. QXRD analysis

QXRD analysis was conducted to understand the relationship between mechanical performance and mineralogy. Figure 5 and Table 3 display the mineral composition change of the pastes in response to different curing scenarios.

GC exhibited a very different mineralogical composition from that of OPC. As expected, alite (C_3S) and belite (C_2S) were the main mineral phases of raw OPC, while rankinite (C_3S_2), belite (C_2S), and gehlenite (C_2AS) were the major constituents of the raw GC.

Compared to the raw OPC, the amount of alite and belite experienced partial reduction after being subjected to both curing methods. A more significant amount of C_3S was consumed after hydration than after carbonation, while C_2S exhibited an opposite trend. This evidently proved that C_2S has a slower hydration process, but a higher carbonation reactivity. A new peak at around 18° presented after one day of hydration curing (OPC-H-1D) of OPC, representing the generation of portlandite. In the carbonation scenario, a characteristic peak centred at 29.3° was significantly enhanced after curing, which was mainly attributed to the formation of calcite ($CaCO_3$).

In contrast, GC pastes exhibited a different mineralogical evolution due to the unique characteristics of its mineral phases. It is known that rankinite and gehlenite have no hydraulic reactivity (Arjunan et al., 1999; Ashraf et al., 2017; Zhutovsky and Shishkin, 2021), and belite has a latent hydraulic property (El-Didamony et al., 1996). Both rankinite and belite have strong carbonation reactivity. After one day of hydration, only a small amount of portlandite was detected, proving a slow hydration process of GC, which was associated with the marginal strength gain within one day of hydration. On the other hand, carbonation curing of GC resulted in a significant reduction of belite and rankinite. This led to the formation of calcite and an amorphous gel. The latter is believed to be a low Ca/Si calcium silicate hydrate (C-S-H). The rapid generation of these two products contributed to the high early strength of the carbonated GC paste. It was found that 14.8% of belite was still present in the cement system after carbonation. Thus, the subsequent strength development of GC after the one day of carbonation was the result of continued hydraulic activation of the remaining unreacted belite phase in the GC.

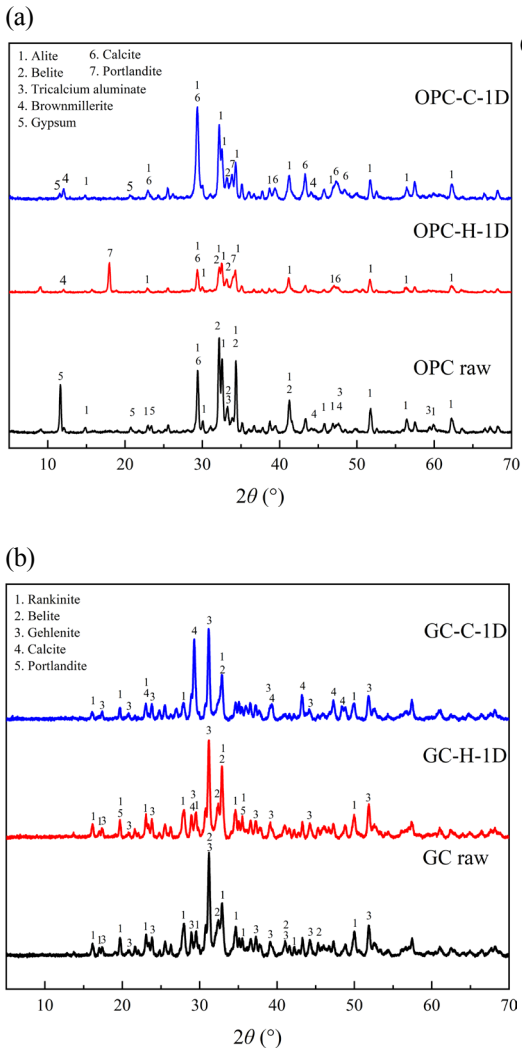

Figure 5. XRD spectra of (a) OPC batch; and (b) GC batch.

Table 3. Mineral compositions of OPC and GC batches at one day by QXRD.

Phases	OPC raw	OPC-H-1D	OPC-C-1D	GC raw	GC-H-1D	GC-C-1D
Alite	54.0	29.1	34.6	-	-	-
Belite	21.6	13.0	9.6	21.0	17.5	14.8
Tricalcium aluminate	5.9	-	-	-	-	-
Brownmillerite	9.2	10.4	9.0	-	-	-
Rankinite	-	-	-	46.1	39.5	12.2
Gehlenite	-	-	-	30.7	26.5	23.6
Gypsum	5.1	-	2.7	-	-	-
Calcite	3.6	7.0	26.4	-	4.8	24.3
Portlandite	-	13.4	0.4	-	5.3	-
Amorphous	0.6	27.1	17.4	2.2	6.3	24.8

3.3. Nanoindentation results of cured cement paste

The indentation modulus mappings of the indented area for the hydration- and carbonation-cured paste specimens at one day are shown in Figure 6. As reported in the literature, the indentation modulus of the primary hydration and carbonation products such as low-density C-S-H, high-density C-S-H, portlandite, and calcite should respectively fall within the following ranges: 13-26 GPa, 26-39 GPa, 40-48 GPa, and 62.5-94 GPa (Sasmal and Anoop, 2019). The unreacted cement clinker typically has a high indentation modulus, as a previous study reported that its average value was around 99.0 GPa (Hu and Li, 2014). Therefore, other than the micro-mechanical strength distribution, the hydration/carbonation product distributions in the cement pastes can also be deduced accordingly.

The red and orange areas with a high modulus can be regarded as the unreacted clinker phase. It was found that the indentation modulus decreased with increasing distance from the centre of the unreacted clinker particles. A common observation for both cement systems was that the amount of residual clinker after being subjected to carbonation curing was less than that of those subjected to hydration curing. This indicated that carbonation curing induced clinker reaction/consumption. The GC-H-1D exhibited the largest area with an indentation modulus of less than 13 GPa compared to other mappings. Such a low modulus could be attributed to voids, which was in agreement with the low compressive strength performance of GC-H-1D. The carbonation curing resulted in a large area of the matrix having a modulus of between 26 and 91 GPa, which might be attributed to the presence of inter-mixed products of calcite and C-S-H gel.

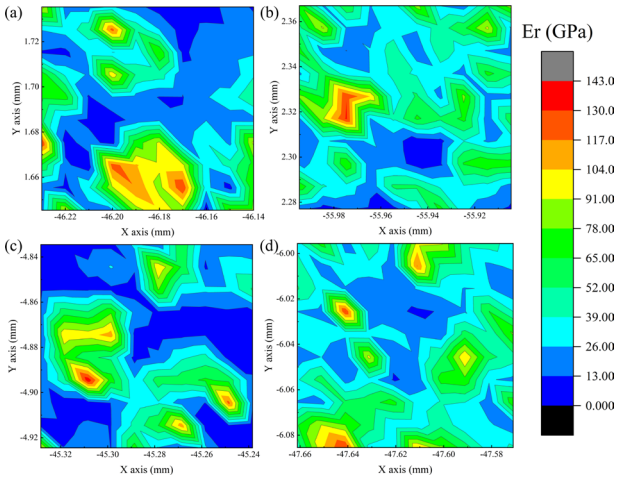

Figure 6. Indentation modulus (E_r) mapping of (a) OPC-H-1D; (b) OPC-C-1D; (c) GC-H-1D; and (d) GC-C-1D.

3.4. FTIR analysis

The FTIR spectra are used to analyse the functional group changes of OPC and GC in the hydration and carbonation curing scenarios. The results are presented in Figure 7. The FTIR spectra of the GC-H-1D were similar to the spectra of the raw GC. The silicate in rankinite and belite together contributed to a characteristic peak of 851 cm^{-1}, corresponding to the asymmetrical stretching vibration of the Si-O bond (Ashraf and Olek, 2016; Lu et al., 2018), which was marked for raw GC and GC-H-1D. The almost identical peak location (851 cm^{-1}) and intensity mean that rankinite and belite were not reactive during the hydration scenario. But the intensity of this peak greatly decreased when GC was subjected to carbonation. Both OPC-C-1D and GC-C-1D exhibited strong and prominent peaks of 873 cm^{-1} and 1425 cm^{-1}, which were attributed to the stretching vibration of the group (CO_3^{2-}) in calcite. In addition, both OPC-C-1D and GC-C-1D displayed a small localised characteristic peak centred at 1080 cm^{-1}, corresponding to

Si-O which resulted from CSH decalcification (Lu et al., 2018). All OPC and GC batches had a broad peak at around 3400 cm^{-1}, resulting from the symmetric stretching vibration of the O-H in CSH gel. A sharp peak of 3640 cm^{-1} for OPC-H-1D, corresponding to the O-H bond of portlandite, was found. The functional group changes identified were consistent with those of the mineralogical analysis by XRD.

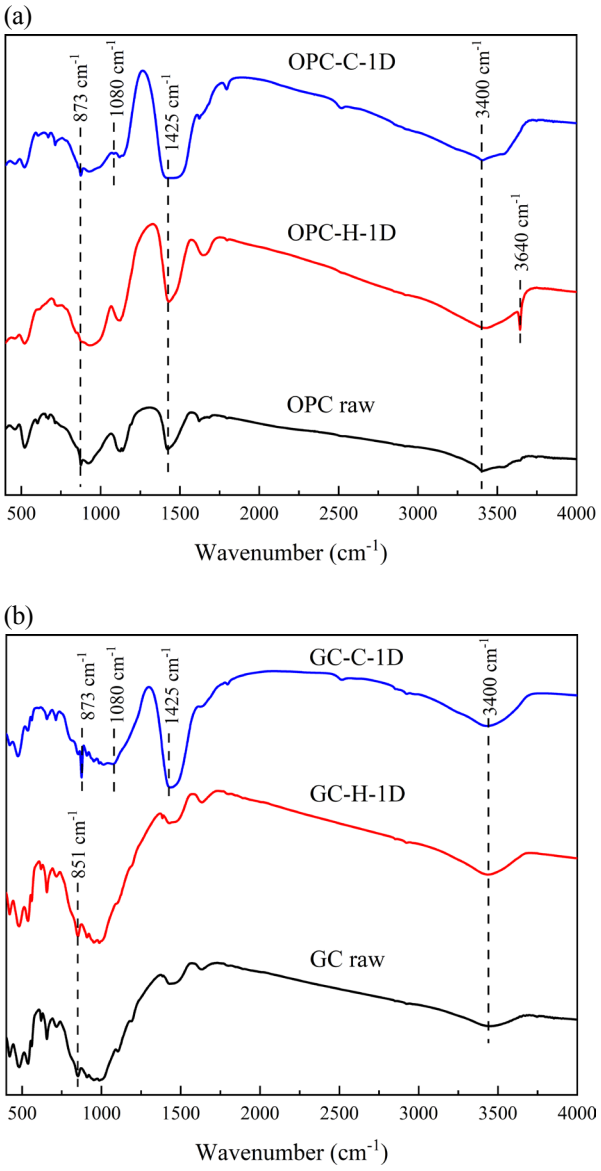

Figure 7. FTIR spectra of (a) OPC batch; and (b) GC batch.

3.5. TGA analysis

Figure 8(a) and (b) display TGA curves for OPC and GC pastes subjected to different curing methods. It is known that carbonation-generated carbonates could have a different level of crystallinity, which can be categorised by their decomposition temperature ranges. The temperature cut-offs were (Ghouleh et al., 2018): free water evaporation between 50°C and 105°C; bonded water decomposition of the hydration product CSH between 105°C and 350°C; bonded water decomposition of portlandite between 350°C and 450°C; and decarbonisation of carbonates between 450 and 800°C.

The OPC-H-1D had a noticeable thermal event caused by portlandite decomposition between 350°C and 450°C. There was a weight loss of 1.7% for raw OPC between 450°C and 800°C, implying that the original content of $CaCO_3$ in the OPC was 3.9%. By performing a calculation based on the TGA results and discounting the original carbonates, the carbonates produced from the carbonation curing were 19.5% for OPC-C-1D, which was smaller than that of GC-C-1D (21.4%). This agreed with the authors' previous research that a marginal carbonate increment could lead to significant strength enhancement due to the effective porosity refinement (Zhang et al., 2021). Therefore, it could be concluded that the GC-C paste produced more carbonates than OPC did after 1 day of carbonation curing, which renders this cement matrix superior mechanical performance.

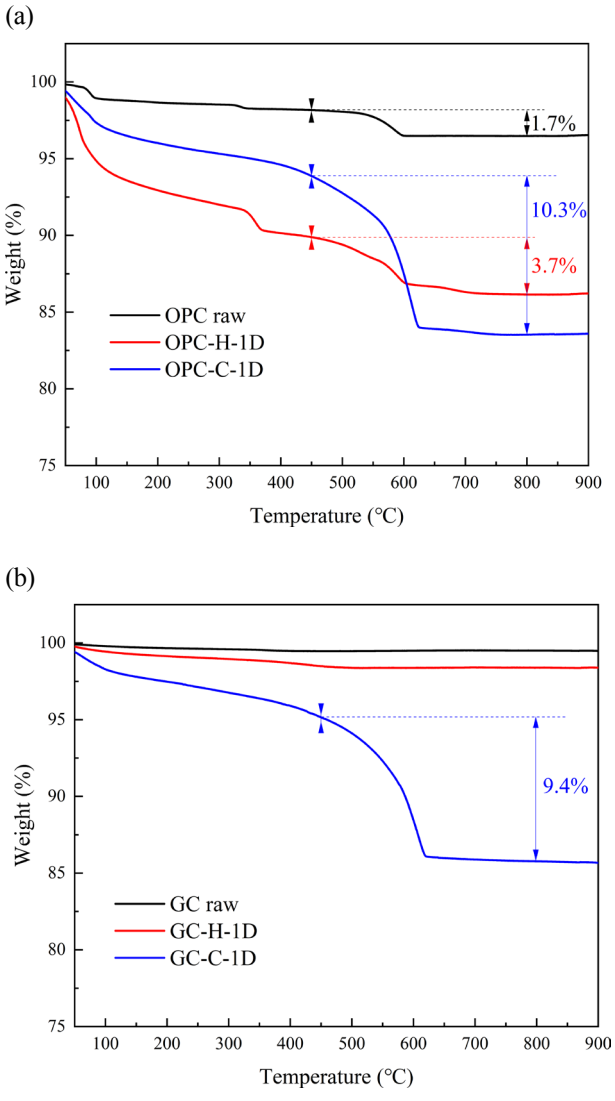

Figure 8. TGA curve of (a) OPC batch; and (b) GC batch, with the weight loss value of the corresponding sample between 450°C and 800°C.

3.6. SEM observation

The fracture surface's morphology of different paste batches was determined by SEM (Figure 9), and the most important carbon-sequestrating mineral - calcium carbonate - was emphasised in this investigation.

Apparently, for both binders, carbonation created a much denser microstructure than that produced by only their hydration counterparts. As highlighted in the zoom-in images, mineral stacking morphologies consisting of small rhombohedral crystals ranging between 650 and 1450 nm can be observed in the carbonated batches regardless of binder type. With the aid of EDX, these minerals could be identified as $CaCO_3$. These small crystals could effectively fill the voids and consequently led to a consolidated matrix. As a microstructure is directly related to macro-performance, this carbonation-induced carbonate consequently enhanced the compressive strength.

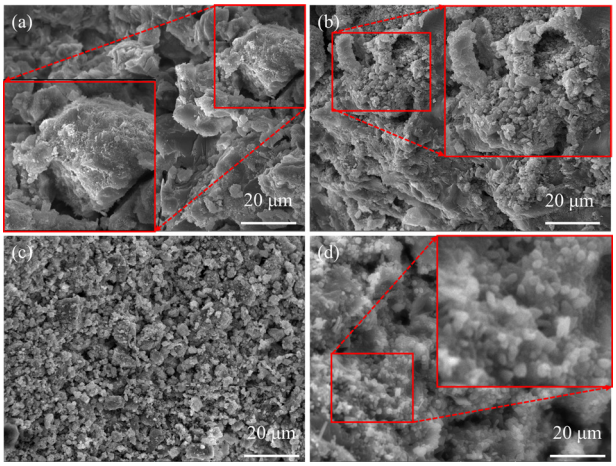

Figure 9. SEM of fracture morphology for (a) OPC-H-1D; (b) OPC-C-1D; (c) GC-H-1D; and (d) GC-C-1D.

3.7. Environmental leaching risk

Using solid wastes as raw materials in cement making requires the environmental suitability of the clinker to be determined. Heavy metals' leaching potential, including that for arsenic, barium, cadmium, chromium, lead, selenium, and silver were determined by TCLP, and the results are summarised in Table 4. The US EPA limitations were adopted as the criteria (AGENCY, U. E. P., 2004) and are presented as well in this table.

It could be concluded that, even for raw GC, the leachate had a far lower heavy metal leaching concentration than the US EPA criteria. As per the principle of cement stabilisation/solidification (Shunda et al., 2022), the intense carbonation behaviour of GC and the corresponding dense microstructure greatly reduced the potential leaching risk of the Ba and Cr, which were the two most significant heavy metals in GC. This test proved that the GC can be used as environmentally friendly cement for sustainable development in construction without heavy metal leaching concerns.

4. Conclusions

In this work, green cement (GC) was produced by sintering using IBA and RCF as the primary raw materials. In addition to the superior mechanical performance, the production of GC could significantly reduce carbon emissions by lowering the sintering temperature, adopting low carbon-embodied raw materials, and sequestrating CO_2 during curing. The main conclusions that can be drawn are as follows:

(1) GC was developed from a raw clinker feed consisting of IBA and RCF and sintered at 1200°C. Its main mineral components were belite, rankinite, and gehlenite, which possessed strong carbonation reactivity and latent hydraulicity.

(2) GC demonstrated a rapid strength gain under carbonation curing, and a one-day compressive strength of 67.8 MPa was achieved, which was even higher than that of OPC hydration control at 60 days. Also, further strength enhancement was observed with aging, and carbonated GC eventually recorded a high strength of 86.4 MPa.

(3) Belite and rankinite were proven to be the carbonation reactive mineral phases in GC, which contributed to the enhanced macro- and micro-mechanical performance, and the carbonation-induced carbonates could effectively densify the microstructure.

(4) TCLP leaching appraisal revealed that this waste-derived GC could be used in construction without heavy metal leaching concerns.

Table 4. Heavy metal concentrations of OPC and GC before and after curing (mg/L).

Materials	As	Ba	Cd	Cr	Pb	Se	Ag
GC raw	0.204	10.04	0.034	3.405	0.18	0.193	0.225
GC-H-1D	0.21	11.195	0.033	2.8	0.185	0.2	0.222
GC-C-1D	0.197	5.43	0.032	1.25	0.17	0.192	0.2
Criteria (AGENCY, U. E. P., 2004)	5.00	100.00	1.00	5.00	5.00	1.00	5.00

Acknowledgments

The authors wish to thank the Hong Kong Research Grants Council (GRF 15226022) and Innovation Technology Fund for their financial support of this research project.

Notes on contributors

Dr Shipeng Zhang is a Research Assistant Professor at The Hong Kong Polytechnic University. Prior to joining the PolyU, he worked as a postdoctoral fellow at McGill University from 2020 to 2021. Dr Zhang's main research interests include the development and characterisation of sustainable construction materials, waste recycling and management, carbon sequestration in concrete, and concrete durability assessment.

Dr Hanxiong Lyu is a Postdoctoral fellow at The Hong Kong Polytechnic University. Dr Lyu received his Ph.D. degree from Harbin Institute of Technology, and he specialises in solid waste management and cement chemistry.

Dr Peiliang Shen is a Research Assistant Professor at The Hong Kong Polytechnic University. Dr Shen's main research interests lie in diverting solid wastes into high-value construction materials.

Dr Zhu Lu is a Postdoctoral fellow at The Hong Kong Polytechnic University. Dr Zhu specialises in high-temperature ceramic materials.

Ir Prof Chi Sun Poon obtained his Ph.D. from Imperial College London. He is currently a chair professor and director of the Research Centre for Environmental Technology and Management at the Civil and Environmental Engineering Department. He has been a Changjiang Scholar Chair Professor since 2017. Ir Prof Poon specialises in the research and development of environmentally friendly construction materials, waste management, waste recycling technologies, and sustainable construction. He has published over 350 papers in international journals. He is a fellow of the Hong Kong Institution of Engineers (HKIE), past chairman of the HKIE Environmental Division and past representative of the HKIE Environmental Discipline. He is also a fellow of the Hong Kong Concrete Institute (HKCI) and is currently the president of the HKCI. He has served on the Advisory Council on the Environment (ACE) and the Council for Sustainable Development, and is currently a member of the advisory committee for the Recycling Fund of the Hong Kong SAR Government.

References

[1] Arjunan P, Silsbee MR and Roy DM (1999). Sulfoaluminate-belite cement from low-calcium fly ash and sulfur-rich and other industrial by-products. *Cement and Concrete Research*, 29, pp. 1305-1311.

[2] Ashraf W and Olek J (2016). Carbonation behavior of hydraulic and non-hydraulic calcium silicates: potential of utilizing low-lime calcium silicates in cement-based materials. *Journal of materials science*, 51, pp. 6173-6191.

[3] Ashraf W, Olek J and Jain J (2017). Microscopic features of non-hydraulic calcium silicate cement paste and mortar. *Cement and Concrete Research*, 100, pp. 361-372.

[4] Baldwin G, Addis R, Clark J and Rosevear A (1997). *Use of industrial by-products in road construction - water quality effects*. London: Construction Industry Research and Information Association.

[5] Cadavid-Giraldo N, Velez-Gallego MC and Restrepo-Boland A (2020). Carbon emissions reduction and financial effects of a cap and tax system on an operating supply chain in the cement sector. *Journal of Cleaner Production*, 275, 122583.

[6] Caldeira K and Wickett ME (2003). Anthropogenic carbon and ocean pH. *Nature*, 425, pp. 365-365.

[7] Clavier KA, Paris JM, Ferraro CC, Bueno ET, Tibbetts CM and Townsend TG (2021). Washed waste incineration bottom ash as a raw ingredient in cement production: Implications for lab-scale clinker behavior. *Resources, Conservation and Recycling*, 169, 105513.

[8] Clavier KA, Paris JM, Ferraro CC and Townsend TG (2020). Opportunities and challenges associated with using municipal waste incineration ash as a raw ingredient in cement production - a review. *Resources, Conservation and Recycling*, 160, 104888.

[9] El-Didamony H, Sharara AM, Helmy IM and El-Aleem SA (1996). Hydration characteristics of β-C_2S in the presence of some accelerators. *Cement and Concrete Research*, 26, pp. 1179-1187.

[10] Gastaldi D, Canonico F, Capelli L, Buzzi L, Boccaleri E and Irico S (2015). An investigation on the recycling of hydrated cement from concrete demolition waste. *Cement and Concrete Composites*, 61, pp. 29-35.

[11] Ghouleh Z, Celikin M, Guthrie RIL and Shao Y (2018). Microstructure of Carbonation-Activated Steel Slag Binder. *Journal of Materials in Civil Engineering*, 30, 04018217.

[12] Hasanbeigi A, Price L and Lin E (2012). Emerging energy-efficiency and CO_2 emission-reduction technologies for cement and concrete production: A technical review. *Renewable and Sustainable Energy Reviews*, 16, pp. 6220-6238.

[13] Hasegawa M (2014). Chapter 3.5 - Thermodynamic Basis for Phase Diagrams. In: SEETHARAMAN, S. (ed.) *Treatise on Process Metallurgy*. Boston: Elsevier.

[14] Hewlett P and Liska M (2019). *Lea's Chemistry of Cement and Concrete*. Elsevier Science.

[15] Hu C and Li Z (2014). Micromechanical investigation of Portland cement paste. *Construction and Building Materials*, 71, pp. 44-52.

[16] Krammart P and Tangtermsirikul S (2004). Properties of cement made by partially replacing cement raw materials with municipal solid waste ashes and calcium carbide waste. *Construction and Building Materials*, 18, pp. 579-583.

[17] Lu B, Shi C and Hou G (2018). Strength and microstructure of CO_2 cured low-calcium clinker. *Construction and Building Materials*, 188, pp. 417-423.

[18] Makarichi L, Jutidamrongphan W and Techato KA (2018). The evolution of waste-to-energy incineration: A review. *Renewable and Sustainable Energy Reviews*, 91, pp. 812-821.

[19] Monkman S and Shao Y (2006). Assessing the carbonation behavior of cementitious materials. *Journal of Materials in Civil Engineering*, 18, pp. 768-776.

[20] Mu Y, Liu Z and Wang F (2019). Comparative Study on the Carbonation-Activated Calcium Silicates as Sustainable Binders: Reactivity, Mechanical Performance, and Microstructure. *ACS Sustainable Chemistry & Engineering*, 7, pp. 7058-7070.

[21] OECD (2019). *Global Material Resources Outlook to 2060 Economic Drivers and Environmental Consequences*. OECD publishing.

[22] Rodriguez N, Murillo R, Alonso M, Martínez I, Grasa G and Abanades JC (2011). Analysis of a Process for Capturing the CO_2 Resulting from the Precalcination of Limestone in a Cement Plant. *Industrial & Engineering Chemistry Research*, 50, pp. 2126-2132.

[23] Saikia NKS and Kojima T (2006). Production of Cement Clinkers from Municipal Solid Waste Incineration (MSWI) Fly Ash. *Waste Management* 27, pp. 1178-1189.

[24] Sasmal S and Anoop MB (2019). Nanoindentation for evaluation of properties of cement hydration products. *Nanotechnology in Eco-efficient Construction*.

[25] Schafer ML, Clavier KA, Townsend TG, Kari R and Worobel RF (2019). Assessment of the total content and leaching behavior of blends of incinerator bottom ash and natural aggregates in view of their utilization as road base construction material. *Waste Management*, 98, pp. 92-101.

[26] Schoon J, De Buysser K, Van Driessche I and De Belie N (2015). Fines extracted from recycled concrete as alternative raw material for Portland cement clinker production. *Cement and Concrete Composites*, 58, pp. 70-80.

[27] Shih PH, Chang, JE and Chiang LC (2003). Replacement of raw mix in cement production by municipal solid waste incineration ash. *Cement and Concrete Research*, 33, pp. 1831-1836.

[28] Shunda L, Jiang X, Zhao Y and Yan J (2022). Disposal technology and new progress for dioxins and heavy metals in fly ash from municipal solid waste incineration: A critical review. *Environ Pollut*, 311, 119878.

[29] Solomon S, Plattner GK, Knutti R and Friedlingstein P (2009). Irreversible climate change due to carbon dioxide emissions. *Proceedings of the National Academy of Sciences*, 106, pp. 1704-1709.

[30] United States Environmental Protection Agency (AGENCY, U. E. P.) (2004). *Test methods for evaluating solid waste, Physical/Chemical Methods (SW 846)*. DC: Office of Solid Waste and Emergency Response Washington.

[31] Xiao J, Ma Z, Sui T, Akbarnezhad A and Duan Z (2018). Mechanical properties of concrete mixed with recycled powder produced from construction and demolition waste. *Journal of Cleaner Production*, 188, pp. 720-731.

[32] Xuan D, Zhan B and Poon CS (2016). Assessment of mechanical properties of concrete incorporating carbonated recycled concrete aggregates. *Cement and Concrete Composites*, 65, pp. 67-74.

[33] Yan K, Sun H, Gao F, Ge D and You L (2020). Assessment and mechanism analysis of municipal solid waste incineration bottom ash as aggregate in cement stabilized macadam. *Journal of Cleaner Production*, 244, 118750.

[34] Zajac M, Irbe L, Bullerjahn F, Hilbig H and Ben Haha M (2022). Mechanisms of carbonation hydration hardening in Portland cements. *Cement and Concrete Research*, 152, 106687.

[35] Zhang S, Ghouleh Z, Liu J and Shao Y (2021). Converting ladle slag into high-strength cementing material by flue gas carbonation at different temperatures. Resources, *Conservation and Recycling*, 174, 105819.

[36] Zhao S, Liu Z and Wang F (2020). Carbonation reactivity enhancement of γ-C_2S through biomineralization. *Journal of CO_2 Utilization*, 39, 101183.

[37] Zhutovsky S and Shishkin A (2021). Recycling of hydrated Portland cement paste into new clinker. *Construction and Building Materials*, 280.